ACS OMEGA

Open Access

http://pubs.acs.org/journal/acsodf

Article

Computational Analysis of Biodegradable Polyester Materials for Biomedical Applications: Investigating Molecular Weight Change due to Hydrolysis

Aeneas Jerron Velu, Pathmathas Thirunavukkarasu, Talal Rahman, Kamal Mustafa, and Dhayalan Velauthapillai*

Cite This: *ACS Omega* 2024, 9, 19108−19116

Read Online

ACCESS | Metrics & More | Article Recommendations

ABSTRACT: Biopolymers have gained significant importance in the field of biomedicine, particularly in addressing organ and tissue loss in living organisms. These polymers exhibit temporary functionality during treatment and undergo biodegradation once their intended purpose is fulfilled. The diverse characteristics of these biopolymers expand their range of applications, albeit necessitating extensive experimentation and a time commitment for thorough investigation. Computational models have emerged as a promising avenue for predictive analysis, complementing traditional experimental methods. In this study, we delve into the degradation dynamics of polyester materials with a specific emphasis on the hydrolysis process. We employed an appropriate reaction diffusion model to unveil the underlying mechanisms governing material weight loss and erosion within a two-dimensional framework for a rectangular slice of the implant. By bridging computational modeling with empirical research, this study provides valuable insights into the behavior of biopolymers, contributing to a deeper understanding of these materials and their potential for advanced biomedical applications. To illustrate this framework's effectiveness, we conducted a case study using experimental data from the literature, focusing on poly(D,L-lactic acid) material.

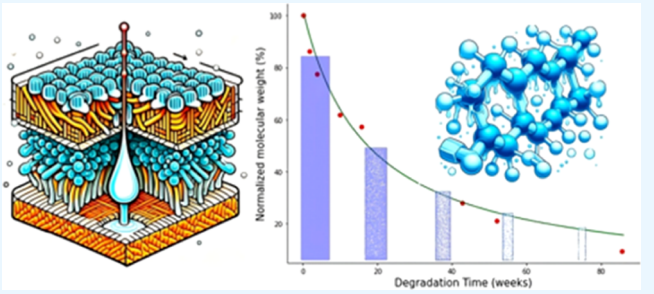

1. INTRODUCTION

In the field of regenerative medicine, various implants, including stents, drug delivery devices,[1] tissue engineering scaffolds, and more, are employed for the controlled release of medications and to offer temporary support to damaged tissues as they heal.[2] The utilization of biopolymers in constructing implants has become increasingly beneficial. Biopolymers can degrade naturally within the biological body while fulfilling their intended function, eliminating the necessity for subsequent surgical removal.[3] Biodegradable polymers utilized as biomaterials for implants like polyesters such as polylactic acid (PLA), polyglycolic acid (PGA), and polycaprolactone (PCL), along with their copolymers, have a wide range of mechanical, chemical, and physical properties with the degradation behavior.[4,5] The properties of these polyesters can be tailored to meet a diverse physiological need and can be customized for patient-specific implants. As a result, these polyesters have become more versatile in their application in various medical implants. For instance, poly(ε-caprolactone), or PCL, is used in both orthopedic implants and controlled drug delivery devices.[6]

A persistent challenge linked to biodegradable polymeric implants is their capability to adequately meet the functional demands of specific target tissues or organs. An ideal polymeric implant should promote cell adhesion and growth while preventing inflammation or immunotoxic responses triggered by either the polymer itself or its degradation byproducts. Furthermore, the implant should possess tunable properties that could facilitate appropriate tissue regrowth.[7,8] To encourage tissue growth, implants are typically designed to imitate healthy tissues in both anatomical and physiological aspects. These necessities enabled construction of complex-shaped implants with pores or lattice microarchitectures.

During clinical applications, polymeric implants are exposed to a biological environment, which is assumed as an aqueous environment. The water molecules penetrated the implant and attacked the backbone of the macromolecular chains in the implant. As a result, short chains (oligomers and monomers) are produced. This process is hydrolysis, and it leads to degradation and erosion of the implant. Degradation is often

Received: December 18, 2023
Revised: March 4, 2024
Accepted: March 7, 2024
Published: April 17, 2024

https://doi.org/10.1021/acsomega.3c10112
ACS Omega 2024, 9, 19108−19116

characterized by the structural and molecular weight changes in a polymeric implant, whereas erosion refers to changes caused by mass loss in degrading the polymeric implant.[9,10] Polyester materials such as PCL, PLA, PGA, and their copolymers undergoing the hydrolysis process and ester bonds are cleaved to form short chains.[11,12] These short chains diffuse out of the polymeric implant which leads to decreased molecular weight, mass loss, and loss of implant's original shape and strength. These are widely used measures to study the degradation and erosion behavior.

There exist two modes of erosion: surface erosion and bulk erosion. Surface erosion is characterized by the gradual loss of mass from the surface of the polymer implants, leading to erosion toward the center of the implant and it is observed in polymers when the rate of degradation exceeds the rate of water diffusion into the implant.[11] On the other hand, bulk erosion takes place when the outward diffusion of monomers from a polymer occurs uniformly as it loses mass. It occurs in a polymer when the rate of diffusion of water into the polymer exceeds the rate of degradation of the macromolecules. Nevertheless, surface and bulk erosion are considered ideal scenarios since in reality, most polymers undergo a combination of both mechanisms.[12] The process alters the size and structure of implants, as they undergo mechanical, chemical, and physical changes during degradation. A range of polymeric materials and compositions have been investigated thoroughly to understand the breakdown of the material. To ascertain the physical and chemical characteristics of the polymers during degradation, the macroscopic changes in molecular weight, fluid concentration of the medium, monomer concentration, crystallinity, and porosity have been investigated.[11,13−15] In a similar fashion, studies on the macroscopic mechanical characteristics of biodegradable polymers and scaffold structures have been carried out to understand their overall behavior during the degradative process.[14,16−18] Nevertheless, understanding the microscopic characteristics of materials remains challenging. In order to ensure proper load-bearing capacity and predict and control the degradation of engineered polymeric implants, it is essential to comprehend the localized changes in physical, chemical, and mechanical properties throughout the degradation of the implant. Although chemical, physical, and mechanical properties of polymeric materials were once believed to be uniform, degradation of polymers causes nonuniform changes to these qualities.[12] The implant's overall structural integrity and tissue growth may be impacted by differences in the material properties and modifications to the geometric shape and size.

Computational models have been developed to account for changes in the spatiotemporal behavior of biodegradable polymer solids caused by changes in their chemical and physical properties. Using coupled partial differential equations, Casalini et al.[10] developed a statistical model for the degradation and drug release of PLGA. The model included reaction kinetics that incorporates the concentration of water, monomers, and oligomers during hydrolytic breakdown. Furthermore, the model discussed the governing differential equations for controlling drug release via erosion. The diffusivity constants for both water and the drug are considered to alter with changes in the molecular weight as the polymer degrades in order to account for the interplay between degradation and erosion. Yu et al.[19] used a cellular automata method to model drug release within multilayer biodegradable polymers in three dimensions, like the probability method used in Gopferich's study. Chen et al.[9] and Sevim and Pan[20] integrated stochastic and differential equations to explain the process of hydrolytic degradation and erosion in drug delivery systems. The differential equations were used to model the mass balance and diffusion of the constituents, while the erosion process was characterized using the probability approach of Gopferich.[12] Based on a phenomenological approach, Wang et al.[21] proposed a model for the degradation of biodegradable polymers. This approach considers the reaction−diffusion processes that involve the concentration of ester bonds of the polymeric materials and monomers and crystallinity in the amorphous polymers. Wang et al.[21] studied the spatial and temporal changes in these components within 3D polymers. However, the model failed to incorporate the erosion process, which enables the integration of alterations in the shape and size of the polymers.

The aim of this study is to gain a comprehensive understanding of several key aspects of hydrolytic degradation and erosion in polyester materials. Specifically, we investigate noncatalytic and autocatalytic rate constants and examine the nature of chain scission. Our approach involves tracking changes in the number-averaged molecular weight of the polyester materials over the degradation period. Additionally, we analyze alterations in the size of polymer implants by considering a rectangular slice of the implant within a two-dimensional (2D) representation. To achieve this, we employ a diffusion model tailored to a polymeric implant system. We address spatial and temporal changes through the application of the finite difference method (FDM). To validate our findings, we utilize experimental data from the literature pertaining to PDLLA material in a bone scaffold context.

2. MODEL

2.1. Hydrolytic Degradation. In clinical applications, the implants immersed in bodily fluids, such as blood, interstitial fluid, transudate, etc., are constructed to fulfill their function placed inside the biological body. Of the 70% of total body water, 55% is composed of intracellular fluid and 45% is composed of extracellular fluid.[22] Due to this, in this study, we assumed that the internal biological environment is an aqueous environment. Hence, the implant experiences hydrolytic degradation, which is the fundamental mechanism for implant degradation. As a consequence of the hydrolytic degradation, the ester bonds in the backbone or side groups of the polymer chains undergo breakdown.[23] Because of the breakdown, long polymer chains turn into short chains, where these short chains diffuse from the implant.[24] The hydrolysis of polyesters is described as follows

$$\mathrm{R-COO-R' + H_2O \rightarrow R-COOH + HO-R'} \quad (1)$$

where R and R′ are long chains that are composed of repeating units of monomers and ester bonds. The water molecules interact with the ester bonds and produce carboxylic acid groups (R−COOH) and alcohol groups (R′−OH). The long chains will then be broken into short chains that contain no more than four monomers in each chain.[25] Properties of polyesters such as molecular weight, strength, toughness, and so on are changed in a different manner during biodegradation. As a result, the spatial changes in polyesters during biodegradation are characterized by heterogeneity even if those properties were initially homogeneous. The primary focus of this paper is to understand the process of hydrolytic

https://doi.org/10.1021/acsomega.3c10112
ACS Omega 2024, 9, 19108−19116

degradation and erosion. Changes in the size and shape of polyester implants can provide a detailed understanding of the degradation. The type of material is one of the influencing factors of degradation. Hence, the degradation periods of PCL, PLA, PGA, and their copolymers are not the same. PLA and PGA degrade considerably more quickly over a few days or months than PCL, which typically takes several years to degrade.[26] Some copolymers show a glassy and rubbery nature. Glassy polymers generally have lower chain mobility and exhibit slower hydrolysis rates, slower water penetration, and slower mechanical changes. On the other hand, rubbery polymers show higher chain mobility, higher hydrolysis rate, rapid water penetration, and increased flexibility and ductility.[25] Depending on the intended use, the right kind of material can be selected to modify the degradation period.

A rectangular slice of the implant considered in 2D space is taken into account in this study in order to comprehend the mechanisms influencing the degradation. The molecular weight of the polyester material is normally distributed in 2D space. The $x-y$ plane is partitioned into a number of cells, which can either be a polymer-filled state or an eroded state. The binary values 1 and 0 represent a polymer-filled state and an eroded state, respectively.[20] This can be represented for an arbitrary cell at position i and j and can be expressed as follows

$$\text{cell state}(i, j) = \begin{cases} 1 & \text{if the cell is material filled} \\ 0 & \text{if the cell is degraded} \end{cases} \tag{2}$$

2.2. Mathematical Model for Degradation. Water penetration is fast compared to the time taken for polymer chain cleavage. After the water penetration, long chains can be broken up into carboxylic acid and alcohol groups. The frequency of this chain breakage is influenced by the mole concentration of ester bonds (C_e) present in the long polymer chain and the mole concentration of short chains (C_{sc}) produced during the chain cleavage. Hence, the rate of change of chain cleavage per unit volume (R_{cs}) is expressed as follows[21]

$$\frac{d}{dt}R_{cs} = k_1 C_e(t = t) + k_2 C_e(t = t)(C_{sc})^m \tag{3}$$

where m is known as the diffusion kinetic index,[25] and k_1 and k_2 are reaction rate constants of noncatalytic and autocatalytic hydrolytic reactions, respectively; the first and second term of the right-hand side of eq 3 represent noncatalytic reaction and autocatalytic reaction, respectively. Also, eq 3 does not account for the presence of water, as it is assumed to be abundant within the polymer. Water molecules first enter the implant at its surface and then move toward its center. Water molecules fill the pore states found throughout the implant as they migrate from its surface to its center. After the water molecules enter the pores, a specific number of monomers and short chains are created as a result of the water molecules' interaction with the ester bonds. This is the initiation of the breakdown process. The size of the monomers and short chains prevents their diffusion from the core to the surroundings, trapping them inside the implant. These trapped monomers and short chains create an acidic environment that accelerates the degradation at the core. On the other hand, short chains created at the surface are immediately released to the surrounding medium, so the degradation is faster at the core than at the surface. Furthermore, Grizzi et al.[27] investigated thin and thick samples made up of the same polymer materials and noticed that thicker samples degraded faster than thin samples.

In general, not every long chain is initially broken into short chains. The following equation shows the short chain, R_{sc}, production rate[20,25]

$$\frac{d}{dt}R_{sc} = \alpha\beta\left(\frac{R_{cs}}{C_e(t = 0)}\right)^{\beta-1}\frac{d}{dt}R_{cs} \tag{4}$$

where R_{sc} is the number of chain cleavage per unit volume, $C_e(t = 0)$ is the initial concentration of ester bonds of a polymer chain, and α and β are empirical parameters that influence the nature of the chain cleavage to produce short chains. Equation 4 can be integrated over the given geometry to obtain the amount of short chain production[25]

$$R_{sc} = \alpha C_e(t = 0)\left(\frac{R_{cs}}{C_e(t = 0)}\right)^{\beta} \tag{5}$$

The mole concentration of ester bonds begins to decrease as the hydrolytic reaction proceeds, but the mole concentration of short chains per unit volume gradually increases. Therefore, the mole concentration of ester bonds at time $t = t$ is given as[25]

$$C_e(t = t) = C_e(t = 0) - R_{sc} \tag{6}$$

These short chains diffuse into the surrounding medium. The rate of this diffusion is expressed as[25]

$$\frac{d}{dt}C_{sc} = \frac{d}{dt}R_{sc} + \frac{\partial\left(D\frac{\partial}{\partial x}C_{sc}\right)}{\partial x} + \frac{\partial\left(D\frac{\partial}{\partial y}C_{sc}\right)}{\partial y} \tag{7}$$

where D is the diffusion coefficient, which controls the diffusion of the short chains and varies with the hydrolysis process.[25] The diffusion coefficient, which is dependent upon porosity, is expressed as

$$D = D_{polymer} + (1.3V_{pore}^2 - 0.3V_{pore}^3)(D_{pore} - D_{polymer}) \tag{8}$$

where $D_{polymer}$ is the diffusion coefficient of short chains in the nondegraded polymer, D_{pore} is the diffusion coefficient of the liquid-filled phase, and V_{pore} is the porosity created due to the diffusion of short chains from the polymeric implant. The porosity can be expressed as[21]

$$V_{pore} = \frac{\alpha C_e(t = 0)\left(\frac{R_{cs}}{C_e(t = 0)}\right)^{\beta} - C_{sc}}{C_e(t = 0)} \tag{9}$$

Because of the increasing porosity, the sudden release of short chains at the end of the degradation process is responsible for additional weight loss. The number-averaged molecular weight (M_n), which is used to measure the weight of the polymer implant, is given as follows[25]

$$M_n = M_{n0}\frac{C_e(t = 0) - R_{sc}}{C_e(t = 0) + DP_0(R_{cs} - R_{sc})} \tag{10}$$

where M_{n0} is the initial molecular weight and DP_0 is the degree of polymerization, which is a measure of the number of monomer units present in a polymer chain.

The erosion that the implant experiences during degradation[28] can be captured using the following rules:[20]

https://doi.org/10.1021/acsomega.3c10112
ACS Omega 2024, 9, 19108−19116

1. The molecular weight within the cell should not exceed a critical threshold.
2. The pixel should be in proximity to an adjacent pixel that has undergone erosion.

The rules can be mathematically expressed for an arbitrary cell at position (i,j) as follows

$$\text{cell state}(i, j) = 0 \text{ if}$$

1. Its molecular weight must be less than its threshold weight $(M_n < M_{wt})$.
2. Its neighboring cell must have been degraded previously.

Once the threshold molecular weight was reached, this erosion model captured the sudden liberation of oligomers.

2.3. Initial and Boundary Conditions. The following were assumed in this study:

(a) The surrounding medium of the implant is water and it is abundant.
(b) The slice of the implant is represented as a 2D grid.
(c) All four sides of the implant are in contact with the medium.
(d) Compared to the implant, the amount of water present in the body is abundant.
(e) There are no chain scissions at the beginning $(R_{sc} = 0)$.

Initially, the molecular weight is distributed normally in the 2D grid, as shown in Figure 1, and the cells at the boundary are

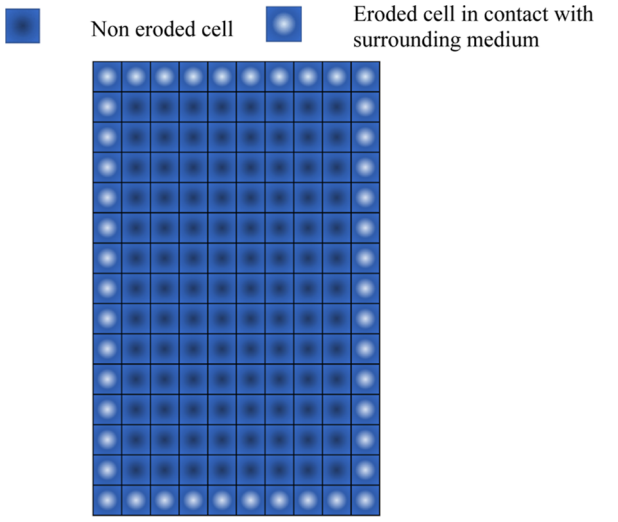

Figure 1. Schematic diagram of 2D implant placed in a medium at the degradation time $t = 0$.

in contact with the medium. Before the degradation starts, the cells that are situated within the grid's borders can be regarded as degraded cells.

An arbitrary cell was considered in the grid at the position (i,j), where i can range from 1 to n_x and j can range from 1 to n_y. Here, n_x and n_y are the total number of cells in the x axis and y axis. Based on this representation, the cells at the boundaries are denoted by $(1,j)$, (n_x,j), $(i,1)$, and (i,n_y).

The initial conditions of inner cell states are given below

$$\text{cell state}(i, j) = 1$$

where $i = [2,n_x - 1]$ and $j = [2,n_y - 1]$.

The concentration of ester bonds at the inner cells is given below

$$C_e(i, j) = C_{e0}$$

where $i = [2,n_x - 1]$ and $j = [2,n_y - 1]$.

The number of short chains and the concentration of short chains are

$$R_{sc} = 0$$

and

$$C_{sc} = 0$$

The initial conditions of outer cells are given as follows:

Cells' states at the boundaries

$$\text{cell state}(1, j) = 0$$

$$\text{cell state}(n_x, j) = 0$$

$$\text{cell state}(i, 1) = 0$$

and

$$\text{cell state}(i, n_y) = 0$$

Concentration of ester bonds at the boundaries

$$C_e(1, j) = 0$$

$$C_e(n_x, j) = 0$$

$$C_e(i, 1) = 0$$

and

$$C_e(i, n_y) = 0$$

2.4. Numerical Methods. The equations presented in Section 2.2 are solved to get a solution by using the FDM. Afterward, the explicit method is applied to the solution to observe temporal changes in the implant.

The temporal part in eq 7 can be written as

$$\frac{d}{dt}C_{sc} = \frac{1}{\Delta t}(C_{sc}^{n+1} - C_{sc}^{n}) \tag{11}$$

The spatial part in eq 7 can be written as given below

$$\frac{\partial}{\partial x_k}\left(D\,\frac{\partial C_{sc}}{\partial x_k}\right) = \frac{D}{\Delta x_k^2}({C_{sc}}_{k-1}^{n} - 2{C_{sc}}_{k}^{n} + {C_{sc}}_{k+1}^{n}) \tag{12}$$

where x_k is an x or a y coordinate.

The mole concentration of short chains per unit volume (C_{short_chain}) and chain cleavage per unit volume $(R_{session})$ can be calculated explicitly as

$$C_{sc}(t + 1) = C_{sc}(t) + \frac{d}{dt}C_{sc} \times \Delta t \tag{13}$$

$$R_{cs}(t + 1) = R_{cs}(t) + \frac{d}{dt}R_{cs} \times \Delta t \tag{14}$$

3. RESULTS AND DISCUSSION

In our study, the model was adopted to validate the experimental data related to molecular weight changes over the specified degradation period. In order to check for changes in the hydrolytic degradation pattern, we assigned a small range of values to the noncatalytic rate constant (k_1) and the autocatalytic rate constant (k_2). The range of k_1 in this instance is 3×10^{-6} to 7×10^{-6} week^{-1}, and the range of k_2 is 0.01−0.05 m^3 mol^{-1} week^{-1}. When k_1 and k_2 were assigned large

https://doi.org/10.1021/acsomega.3c10112
ACS Omega 2024, 9, 19108−19116

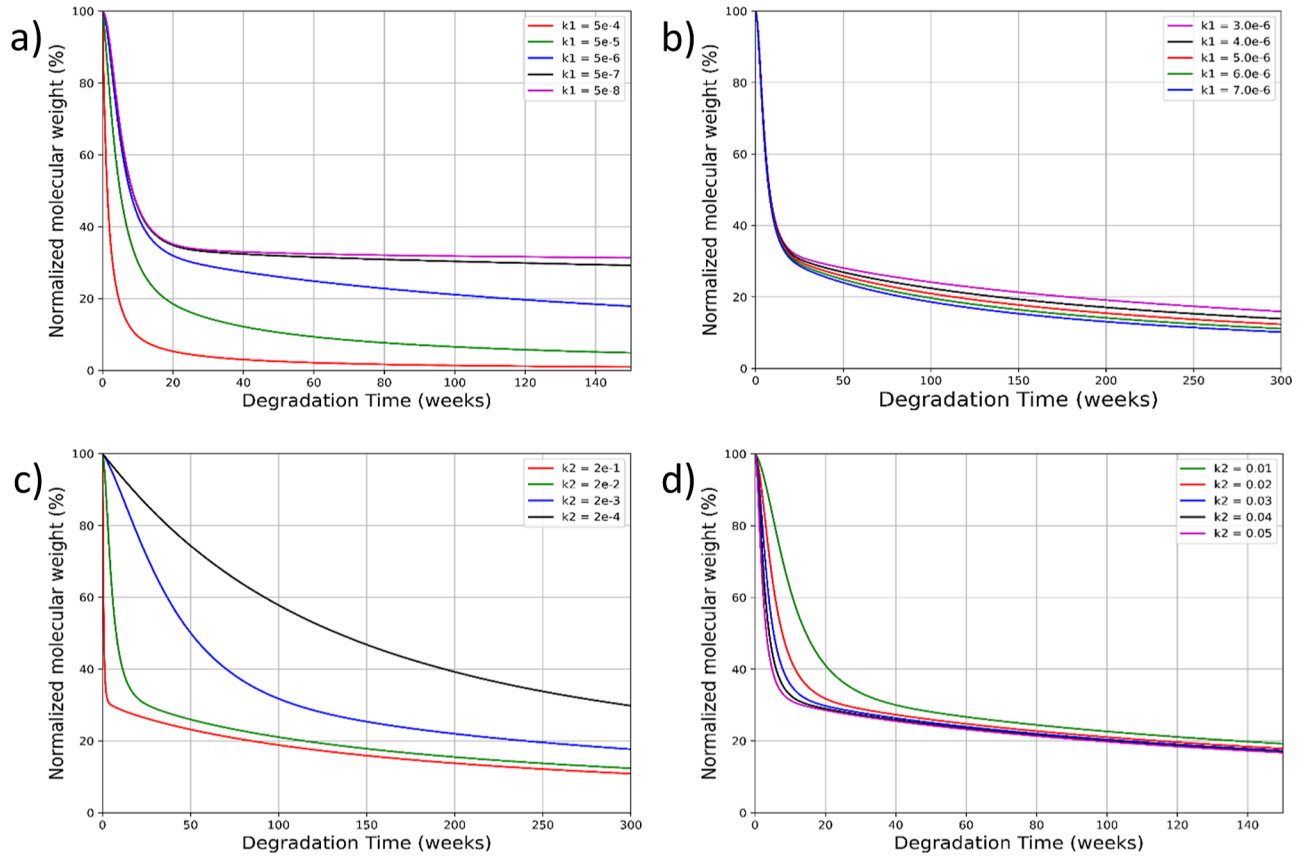

Figure 2. Normalized molecular weight change with time. (a) Large change in the noncatalytic reaction constant (k_1), (b) small change in the noncatalytic reaction constant (k_1), (c) large change in the autocatalytic reaction constant (k_2), and (d) small change in the autocatalytic reaction constant (k_2).

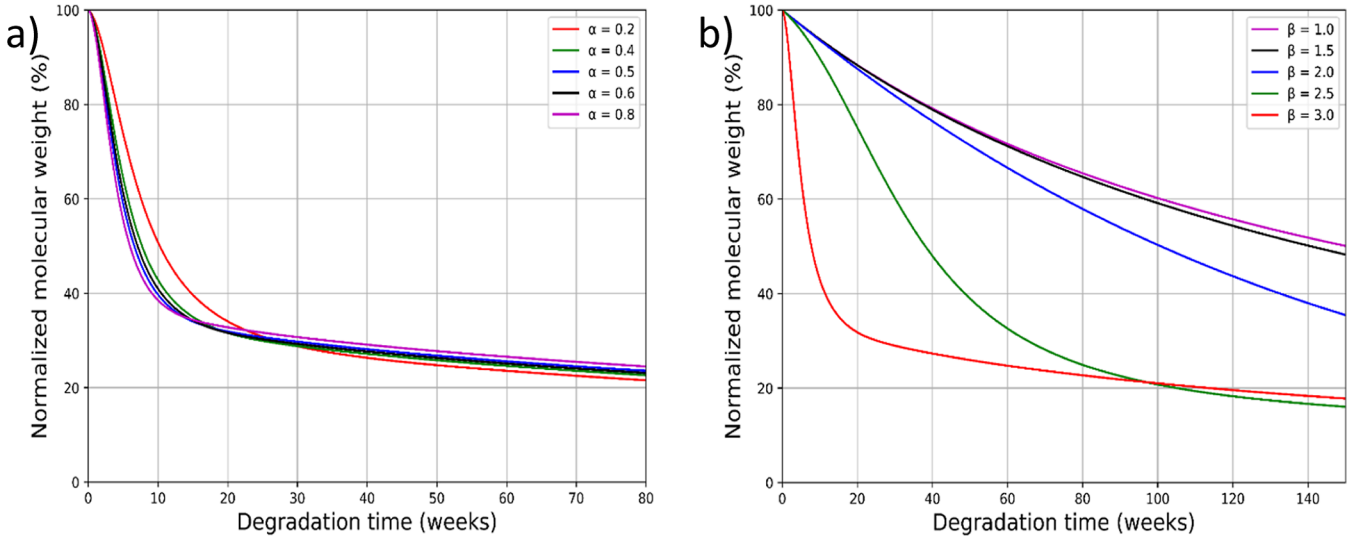

Figure 3. Normalized molecular weight change with (a) α and (b) β values in eq 4.

values, a degradation pattern was also observed. In this case, k_1's range is 5×10^{-8} to 5×10^{-4} week^{-1}, and k_2's range is 2×10^{-4} to 2×10^{-1} $\sqrt{\text{m}^3\ \text{mol}^{-1}}$ week^{-1}.

Empirical parameters α and β, which characterize the nature of cleavage according to eq 4, have been given numerical values so that their impact on the rate of degradation can be observed. The range of α in this instance is 0.2−0.8, and the range of β is 1−3. Throughout these analyses, the remaining parameters were held constant, allowing us to investigate the degradation patterns by varying the specific parameter values.

3.1. Noncatalytic and Autocatalytic Reaction Rate Constants k_1 and k_2. The breakdown patterns of polyester materials that may undergo both noncatalytic and autocatalytic reactions during the hydrolytic degradation process, and which have different k_1 and k_2 values, are shown in Figure 2. It was found that abrupt shifts in molecular weight happened for all

https://doi.org/10.1021/acsomega.3c10112
ACS Omega 2024, 9, 19108−19116

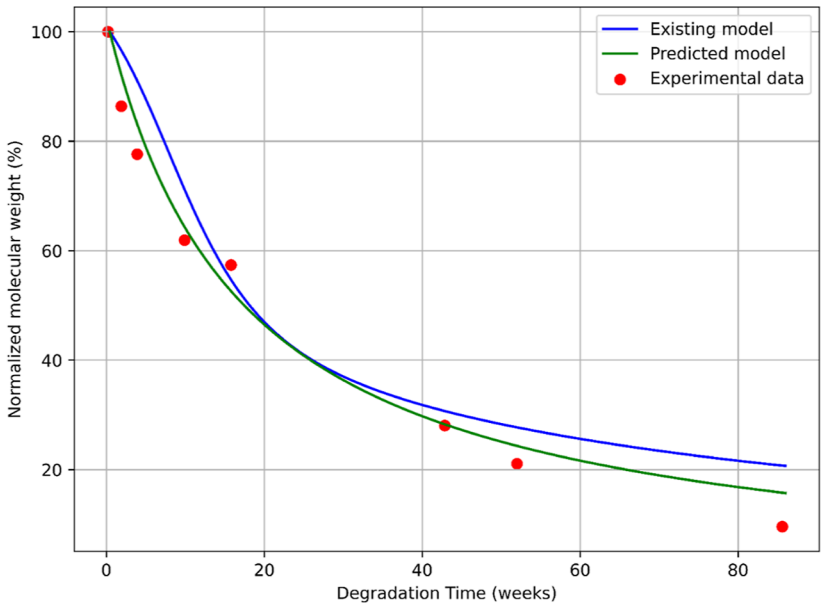

Figure 4. Predicted results of this paper and the experimental data of Blaker et al.[29] for normalized molecular weight over the scaffold as a function of time.

materials only during the initial phases of degradation. In contrast, with the exception of the first phase, molecular weight changes happened gradually.

Figure 2a illustrates how, in comparison to other values of k_1, there is a sudden decrease in the molecular weight at the higher reaction rate of $k_1 = 7 \times 10^{-6}$ week^{-1} because of degradation. In this specific case, the molecular weight loss is almost 80%. After that, the molecular weight gradually decreases over time and reaches saturation after 150 weeks. For lower reaction rates, the molecular weight decreases and reaches saturation much earlier compared to the higher reaction rate, while more than 20% of the initial molecular weight is yet to be degraded.

Figure 2b illustrates the sudden drop in the molecular weight caused by degradation for all values of k_1 that coincide. For every value of k_1, there was a nearly 65% decrease in the molecular weight in this case. For the value of $k_1 = 7 \times 10^{-6}$ week^{-1} in this instance, there was a nearly 70% reduction in the molecular weight loss. After that, the implant's molecular weights gradually drop in accordance with the k_1 values.

Figure 2c illustrates the sudden drop in the implant's molecular weight caused by degradation, which corresponds to values of $k_2 = 0.2$ and $0.02\ \sqrt{\text{m}^3\ \text{mol}^{-1}}\ \text{week}^{-1}$ in comparison to other values of k_2. Following that, for all values of k_2, the molecular weight gradually decreases.

As illustrated in Figure 2d, sudden molecular weight losses of approximately 65% occur for all values of k_2 as a result of implant degradation.

Figure 2 illustrates how the values of reaction rates k_1 and k_2, which are dependent on the temperature, concentration of reactants, surface area, pressure, and composition of the material, are crucial in the implant's degradation.

3.2. Empirical Parameters α and β. Empirical parameters α and β can determine if a chain session is a random session or an end session. Figure 3 illustrates how variations in α and β values led to the molecular weight loss in the implant. The molecular weight loss is generally not the same for α and β values; however, it demonstrated almost the same sudden decrease for $\alpha = 0.2$ and $\beta = 1$. Higher values of α predominate in the initial degradation. On the other hand, the later degradation process was dominated by low α values. Conversely, lower values of β predominate in the initial differentiation process, and high β values governed the degradation process in a later period.

3.3. Blaker's Experimental Investigation for the Bone Scaffold. In our investigation, we employed the model to determine the suitable parameters required for predicting the material's lifetime within the context of our study. This involved adjusting the parameters specified in eqs 3 and 4 to account for their varying nature. The number-averaged molecular weight as a function of time for in vitro bone scaffold disintegration was investigated experimentally by Blaker et al.[29] This experiment was carried out over a 600 day period at a temperature of 37 °C using simulated body fluid. The mathematical model used in this work is explicitly tested using the molecular weight data. Blaker et al. investigated how PDLLA and PDLLA/Bioglass composites degraded over time. Even though the polymer shows a glassy nature, during the first 12 weeks, the molecular weight of the neat PDLLA showed a significant drop.

3.4. Model Validation. For the model we used in our investigation, k_1, k_2, α, and β have specific values assigned to them. As a result, the degradation pattern we obtained and the one obtained experimentally were nearly identical. Blaker's experimental results are taken into consideration because they employed pure polyester (PDLLA) as the implant material and conducted a 600 day study in order to gather comprehensive data. It is crucial to remember that the main ingredients of the model we used and the one Sevim published in 2018 are essentially the same. However, there are differences in the values of k_1, k_2, α, and β between the model that we employed and the one that Sevim published. Furthermore, model parameters associated with the implant's initial state of degradation are tabulated in Table 1.

Based on our model and Sevim's model, there are notable differences in the molecular weight loss that occurred in the period of 0−20 weeks. Nonetheless, the molecular weight loss

https://doi.org/10.1021/acsomega.3c10112
ACS Omega 2024, 9, 19108−19116

Table 1. Parameters Used to Obtain the Model Fit for the Experimental Data in Figure 4

model parameters	values	units
M_{mean}	1.3×10^5	g mol−1
M_{n,st_dev}	1.3×10^3	g mol−1
M_{unit}	72[20]	g mol−1
m	0.5[21]	no unit
α	0.2	no unit
β	3	no unit
$C_{e,0}$	20,615[20]	mol m^{-3}
M_{wt}	4.0×10^4	g mol^{-1}
D_{pore}	1.0×10^{-5}[20]	m^2 $week^{-1}$
k_1	3.0×10^{-5}	$week^{-1}$
k_2	2.0×10^{-1}	m^3 mol^{-1} $week^{-1}$
$D_{polymer}$	5.0×10^{-15}[20]	m^2 $week^{-1}$

obtained from both models varied similarly over the course of 20 and 30 weeks. After 30 weeks of degradation, the molecular weight loss obtained from each model began to gradually diverge.

The values of the model parameters tabulated in Table 1 were used to determine the erosion process that occurred over the period, as shown in Figure 5. The water molecules that entered the implant attacked the molecules at the core. As a result of the chain session, carboxylic acid and alcohol groups are produced. Because the sizes of the aforementioned components are larger than the pore networks through which the water molecules enter, the components are trapped in the core. This phenomenon increases the acidity of the environment, which leads to bulk erosion. Grizzi et al.[27] observed this type of erosion pattern for thick implants. As shown in Figure 5, the percentage of erosion over the degradation period is given. This provides information on the bulk erosion, the blue-colored region representing the polymer region and the white-colored region representing the degraded region. According to the comparison of Figures 4 and 5, 50% of the erosion occurred within 20 weeks, while 80% occurred after 60 weeks. This observation shows that the rate of degradation was higher in the early stages than it was at the end.

4. CONCLUSIONS

This work demonstrates the successful integration of differential equations related to reaction−diffusion, empirical principles, and the FDM to effectively describe the degradation behavior of bulk polymers. A comprehension of the hydrolytic degradation process is achieved by considering the interplay between hydrolytic chain scission, autocatalytic effects, short chains' diffusion, and bulk erosion. Furthermore, the 2D model representation is validated by comparing it with experimental data for PDLLA material in a bone scaffold. This modeling technique serves as a valuable tool for accurately defining and predicting the degradation behavior of polyesters, enhancing our understanding of their real-world performance. These

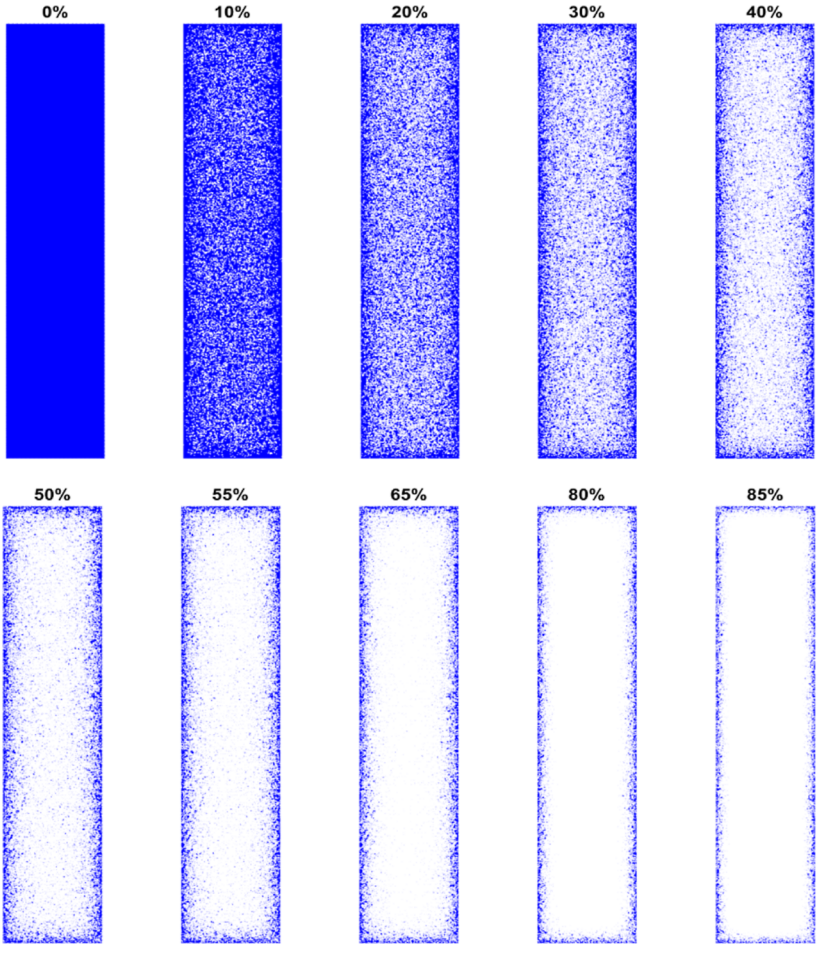

Figure 5. Erosion progress over the period of degradation.

https://doi.org/10.1021/acsomega.3c10112
ACS Omega 2024, 9, 19108−19116

insights can be applied to digitally design innovative biodegradable implants for materials with similar composites and functional groups utilizing the same approach. This approach allows for the engineering of implants with controlled degradation while maintaining the desired mechanical properties, making it a feasible endeavor.

AUTHOR INFORMATION

Corresponding Author

Dhayalan Velauthapillai − *Department of Computer Science, Electrical Engineering and Mathematical Sciences, Western Norway University of Applied Sciences, Bergen 5063, Norway*; orcid.org/0000-0002-4162-7446; Email: dhayalan.velauthapillai@hvl.no

Authors

Aeneas Jerron Velu − *Clean Energy Research Laboratory, Department of Physics, University of Jaffna, Jaffna 40000, Sri Lanka; Department of Computer Science, Electrical Engineering and Mathematical Sciences, Western Norway University of Applied Sciences, Bergen 5063, Norway*

Pathmathas Thirunavukkarasu − *Clean Energy Research Laboratory, Department of Physics, University of Jaffna, Jaffna 40000, Sri Lanka*

Talal Rahman − *Department of Computer Science, Electrical Engineering and Mathematical Sciences, Western Norway University of Applied Sciences, Bergen 5063, Norway*

Kamal Mustafa − *Center of Translational Oral Research-Tissue Engineering, Department of Clinical Dentistry, Faculty of Medicine, University of Bergen, Bergen 5009, Norway*

Complete contact information is available at: https://pubs.acs.org/10.1021/acsomega.3c10112

Notes

The authors declare no competing financial interest.

ACKNOWLEDGMENTS

This research was funded by the Capacity Building and Establishment of a Research Consortium (CBERC) Project (grant no. LKA-3182-HRNCET) and Higher Education and Research Collaboration on Nanomaterials for Clean Energy Technologies (HRNCET) Project (grant no. NORPART/2016/10237).

REFERENCES

(1) Liechty, W. B.; Kryscio, D. R.; Slaughter, B. V.; Peppas, N. A. Polymers for drug delivery systems. *Annu. Rev. Chem. Biomol. Eng.* **2010**, *1*, 149−173.

(2) Zhang, H.; Zhou, L.; Zhang, W. Control of scaffold degradation in tissue engineering: A review. *Tissue Eng.* **2014**, *20* (5), 492−502.

(3) Treiser, M.; Abramson, S.; Langer, R.; Kohn, J. Degradable and Resorbable Biomaterials. *Biomaterials Science: An Introduction to Materials*, 3rd ed.; Elsevier Inc.: Amsterdam, 2013.

(4) Rodenas-Rochina, J.; Vidaurre, A.; Castilla Cortázar, I.; Lebourg, M. Effects of hydroxyapatite filler on long-term hydrolytic degradation of PLLA/PCL porous scaffolds. *Polym. Degrad. Stab.* **2015**, *119*, 121−131.

(5) Silva, M.; Ferreira, F. N.; Alves, N. M.; Paiva, M. C. Biodegradable polymer nanocomposites for ligament/tendon tissue engineering. *J. Nanobiotechnol.* **2020**, *18* (1), 23.

(6) Lyu, S.; Untereker, D. Degradability of Polymers for Implantable Biomedical Devices. *Int. J. Mol. Sci.* **2009**, *10*, 4033−4065.

(7) Middleton, J. C.; Tipton, A. J. Synthetic Biodegradable Polymers as Orthopedic Devices. *Biomaterials* **2000**, *21* (23), 2335−2346.

(8) Freed, L. E.; Vunjak-Novakovic, G.; Biron, R. J.; Eagles, D. B.; Lesnoy, D. C.; Barlow, S. K.; Langer, R. Biodegradable polymer scaffolds for tissue engineering. *Nat. Biotechnol.* **1994**, *12* (7), 689−693.

(9) Chen, Y.; Zhou, S.; Li, Q. Mathematical Modeling of Degradation for Bulk-Erosive Polymers: Applications in Tissue Engineering Scaffolds and Drug Delivery Systems. *Acta Biomater.* **2011**, *7*, 1140−1149.

(10) Casalini, T.; Rossi, F.; Lazzari, S.; Perale, G.; Masi, M. Mathematical Modeling of PLGA Microparticles: From Polymer Degradation to Drug Release. *Mol. Pharmaceutics* **2014**, *11*, 4036−4048.

(11) Burkersroda, F. v.; Schedl, L.; Göpferich, A. Why Degradable Polymers Undergo Surface Erosion or Bulk Erosion. *Biomaterials* **2002**, *23* (21), 4221−4231.

(12) Göpferich, A. Mechanisms of Polymer Degradation and Erosion. *Biomaterials* **1996**, *17* (2), 103−114.

(13) Gentile, P.; Chiono, V.; Carmagnola, I.; Hatton, P. V. An Overview of Poly(lactic-*co*-glycolic) Acid (PLGA)-Based Biomaterials for Bone Tissue Engineering. *Int. J. Mol. Sci.* **2014**, *15*, 3640−3659.

(14) Perron, J. K.; Naguib, H. E.; Daka, J.; Chawla, A.; Wilkins, R. A study on the effect of degradation media on the physical and mechanical properties of porous PLGA 85/15 scaffolds. *J. Biomed. Mater. Res., Part B* **2009**, *91B* (2), 876−886.

(15) Dunn, A. S.; Campbell, P. G.; Marra, K. G. The influence of polymer blend composition on the degradation of polymer/hydroxyapatite biomaterials. *J. Mater. Sci.: Mater. Med.* **2001**, *12*, 673−677.

(16) Ebrahimian-Hosseinabadi, M.; Ashrafizadeh, F.; Etemadifar, M.; Venkatraman, S. S. Evaluating and Modeling the Mechanical Properties of the Prepared PLGA/Nano-BCP Composite Scaffolds for Bone Tissue Engineering. *J. Mater. Sci. Technol.* **2011**, *27*, 1105−1112.

(17) Yang, F.; Cui, W.; Xiong, Z.; Liu, L.; Bei, J.; Wang, S. Poly(l,l-lactide-co-glycolide)/tricalcium phosphate composite scaffold and its various changes during degradation in vitro. *Polym. Degrad. Stab.* **2006**, *91*, 3065−3073.

(18) Breche, Q.; Chagnon, G.; Machado, G.; Girard, E.; Nottelet, B.; Garric, X.; Favier, D. Mechanical behaviour's evolution of a PLA-b-PEG-b-PLA triblock copolymer during hydrolytic degradation. *J. Mech. Behav. Biomed. Mater.* **2016**, *60*, 288−300.

(19) Yu, R.; Chen, H.; Chen, T.; Zhou, X. Modeling and simulation of drug release from multi-layer biodegradable polymer microstructure in three dimensions. *Simul. Modell. Pract. Theory* **2008**, *16* (1), 15−25.

(20) Sevim, K.; Pan, J. A model for hydrolytic degradation and erosion of biodegradable polymers. *Acta Biomater.* **2018**, *66*, 192−199.

(21) Wang, Y.; Pan, J.; Han, X.; Sinka, C.; Ding, L. A Phenomenological Model for the Degradation of Biodegradable Polymers. *Biomaterials* **2008**, *29*, 3393−3401.

(22) Gauttam, N.; Singh, S. P.; Khinchi, M. P.; Nama, N.; Jain, S. Different Body Fluids: An Overview. *Asian J. Pharm. Res. Dev.* **2017**, *5* (1), 1−9.

(23) He, Y.; Li, H.; Xiao, X.; Zhao, X. Polymer Degradation: Category, Mechanism and Development Prospect. *E3S Web Conf.* **2021**, *290*, 01012.

(24) Buchanan, F. J. *Degradation Rate of Bioresorbable Materials: Prediction and Evaluation*; Woodhead: Cambridge, 2008.

(25) Pan, J. *Modelling Degradation of Bioresorbable Polymeric Medical Devices*; Woodhead: Camridge, 2015.

(26) Gunatillake, P. A.; Adhikari, R. Biodegradable synthetic polymers for tissue engineering. *Eur. Cells Mater.* **2003**, *5*, 1−16.

(27) Grizzi, I.; Garreau, H.; Li, S.; Vert, M. Hydrolytic Degradation of Devices Based on Poly(Dl-Lactic Acid) Size-Dependence. *Biomaterials* **1995**, *16* (4), 305−311.

(28) Göpferich, A. Erosion of composite polymer matrices. *Biomaterials* **1997**, *18* (5), 397−403.

(29) Blaker, J. J.; Nazhat, S. N.; Maquet, V.; Boccaccini, A. R. Long-term in vitro degradation of PDLLA/Bioglass® bone scaffolds in acellular simulated body fluid. *Acta Biomater.* **2011**, *7*, 829−840.

https://doi.org/10.1021/acsomega.3c10112
ACS Omega 2024, 9, 19108−19116